



Investigation of Copper Agglomeration at Elevated Temperatures

Ching-Yu Yang and J. S. Chen^{*,z}

Department of Materials Science and Engineering, National Cheng Kung University, Tainan, Taiwan

In this work, the agglomeration behavior of copper thin films after high temperature annealing was investigated. Cu (200 or 50 nm)/Ta (10 nm, or no Ta)/Ta_N (50 nm)/Ta (10 nm) layers were deposited onto SiO₂ (270 nm)/Si substrates by magnetron sputtering. All samples were annealed in vacuum at temperatures ranging from 400 to 800°C. The sheet resistance, phases, surface morphology, elemental depth profiles, and chemical binding states were investigated by four-point probe, θ -2 θ X-ray diffraction, scanning electron microscopy (SEM), Auger electron spectroscopy, and X-ray photoelectron spectroscopy (XPS). Experimental results revealed that 50 nm thick copper films deposited directly onto Ta_N agglomerated after annealing at 600°C. No copper agglomeration was observed for 200 nm thick copper films even after annealing at 800°C. It is also observed that copper agglomeration was prevented while a Ta layer was interposed between Cu and Ta_N. SEM and XPS results showed that, with a Ta interposed interlayer, copper grain growth was slowed down and Ta out-diffused to the copper surface to form a TaO_x layer. The slow grain growth rate of copper and forming of TaO_x cap layer are believed to be the main reasons for preventing copper agglomeration.

© 2003 The Electrochemical Society. [DOI: 10.1149/1.1627350] All rights reserved.

Manuscript submitted August 28, 2002; revised manuscript received June 4, 2003. Available electronically November 3, 2003.

With the development of ultralarge-scale integration (ULSI) circuits, low resistivity and good electromigration resistance have become critical requirements for interconnect material. Compared to the conventional Al-based interconnect, copper has lower resistivity (Al: 2.7 $\mu\Omega$ cm, Cu: 1.7 $\mu\Omega$ cm) and better electromigration resistance.^{1,2} However, copper also has several disadvantages such as fast diffusion into Si³ and SiO₂,⁴ and poor adhesion⁵ to most dielectric materials. Therefore, choosing a suitable diffusion barrier/adhesion promoter becomes an increasingly important issue. Refractory metals⁶⁻⁸ and their nitrides⁹⁻¹¹ are recognized as attractive diffusion barrier materials due to their thermal stability and electrical property. Among them, tantalum and its nitrides attract more attention because of their low resistivity and inactivity to copper.^{12,13} Besides, tantalum and its nitrides have excellent adhesion to Si and SiO₂. Hence, the material may serve as both diffusion barrier and adhesion promoter to dielectric layers of copper interconnection.

However, it is observed that after high temperature annealing, copper films on Ta_N barrier may exhibit agglomeration.¹¹ Copper agglomeration was also observed for copper films on other barrier materials, such as TiN,⁹ Ti-Si-N,¹⁴ TiB₂,¹⁵ WC,¹⁶ and MoN,¹⁰ after high temperature annealing. Although copper agglomeration has been reported in the literatures, most of them mainly concern the interfacial reaction between copper and diffusion barriers. In these studies, the cause for agglomeration of copper thin films was simplified to the high copper/barrier interface energy or low barrier surface energy, so that the copper films will become agglomerated to expose the underneath barrier layer.

To avoid the copper agglomeration, it has been reported that copper became less agglomerated when deposited on Ta barrier than on Ta_N.¹⁷ However, the thermal stability of pure Ta is not so good as Ta_N for acting as a diffusion barrier.¹³ In order to modify the surface of Ta_N but keep it as the main barrier layer, we interposed a thin Ta (10 nm) interlayer between copper and Ta_N and the effect of the Ta interlayer on copper agglomeration was investigated. In addition, the influence of the copper film thickness on agglomeration was studied also because it has been shown that copper films were less likely to agglomerate when they were relatively thick.¹⁸ The Cu, Ta, and Ta_N layers were deposited on SiO₂-covered Si substrates to simulate the interconnection system. The multilayer structures were annealed at various temperatures to examine the agglomeration behavior of copper films.

Experimental

(100) oriented n-type silicon wafers were used as substrates in experiments. After cleaning, the wafers were thermally oxidized at 1050°C in oxygen atmosphere to grow a 270 nm thick SiO₂ layer. Ta_N (50 nm)/Ta (10 nm) layers were deposited onto the SiO₂/Si substrates and followed by a Cu film (200 or 50 nm), with or without a 10 nm thick Ta interlayer. The stacking sequences of the deposited films are Cu (200 or 50 nm)/Ta (10 nm, with or without)/Ta_N (50 nm)/Ta (10 nm)/SiO₂ (270 nm)/Si. The base pressure of the sputtering chamber was 2.5×10^{-6} Torr. The working pressure was set at 4×10^{-3} Torr for Cu deposition, and 7×10^{-3} Torr for Ta and Ta_N deposition. The multilayer structure was deposited sequentially without breaking the vacuum and a negative dc bias of 100 V was applied to the substrate. All samples were subsequently annealed at various temperatures ranging from 400 to 800°C, at a pressure of 3×10^{-5} Torr for 30 min.

Regarding to the sample characterization, sheet resistance was measured by four-point probe. θ -2 θ X-ray diffraction (XRD, θ -2 θ , Rigaku D-Max-IV) was used for identifying the phases of multilayers. Scanning electron microscopy (SEM, Philips XL-40FEG) was employed to observe the morphological evolution of the sample surfaces after annealing. Compositional depth profiles were measured by Auger electron spectroscopy (AES, VG MicroLab 310D), and X-ray photoelectron spectroscopy (XPS, VG ESCA-210) was applied to examine chemical bonding states of the sample surfaces after annealing.

Results and Discussion

The basic multilayer structure in this study was Cu/Ta_N/Ta/SiO₂/Si. The Ta layer between Ta_N and SiO₂ served as a glue layer to ensure a good adhesion. The Cu film thickness was set to be 200 or 50 nm. Another Ta layer would, or would not, be interposed between Cu and Ta_N to modify the interface. Therefore, four different structures, Cu (200 nm)/Ta_N/Ta/SiO₂/Si, Cu (50 nm)/Ta_N/Ta/SiO₂/Si, Cu (200 nm)/Ta/Ta_N/Ta/SiO₂/Si, and Cu (50 nm)/Ta/Ta_N/Ta/SiO₂/Si, were explored in the experiments. Figure 1 shows the variation of sheet resistance with annealing temperature for the four structures. It was observed that the sheet resistance of the structures with thick copper (200 nm) remains stable after annealing up to 800°C. However, the sheet resistance of Cu (50 nm)/Ta_N/Ta/SiO₂/Si increased abruptly after annealing at 600°C, and the sheet resistance continuously increased with increasing temperature. On the other hand, with a 10 nm thick Ta layer interposed between the 50 nm thick Cu and Ta_N, the sheet resistance remains low after annealing up to 700°C and then increased slightly after annealing at

* Electrochemical Society Active Member.

^z E-mail: jenschen@mail.ncku.edu.tw

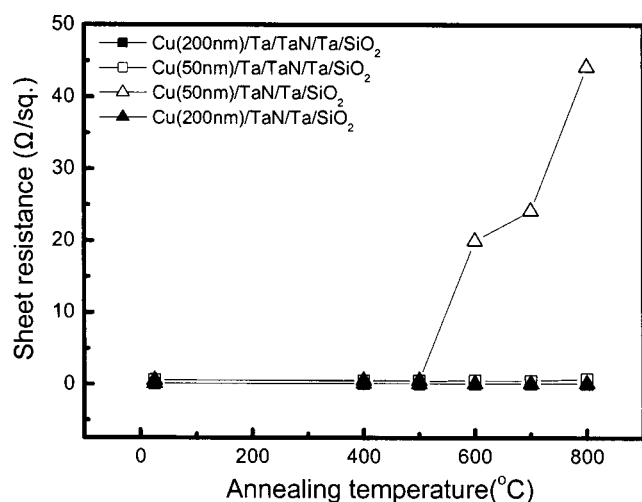


Figure 1. Sheet resistance as a function of annealing temperature for Cu (200 nm)/Ta/TaN/Ta/SiO₂/Si, Cu (200 nm)/Ta/TaN/Ta/SiO₂/Si, Cu (50 nm)/Ta/TaN/Ta/SiO₂/Si, and Cu (50 nm)/Ta/TaN/Ta/SiO₂/Si structures.

800°C. In order to understand the difference in the sheet resistance variation for these four systems, material characteristics of these samples were examined as follows.

Figure 2 presents the θ -2 θ XRD spectra of Cu (50 nm)/Ta/TaN/SiO₂/Si samples, as deposited and after annealing at various temperatures. The as-deposited sample exhibits TaN(111), Cu(111), and Cu(200) diffraction peaks. After annealing, the Cu(111) peak became sharper, which implies grain growth of copper upon annealing and the TaN(200) diffraction peak was observed after annealing at 600°C. Also, TaN(111) peaks of the annealed samples shifts to the right slightly. It may be attributed to the mixing of TaN/Ta layers, which results in the reduction of lattice parameter for the TaN phase. No new phases were formed in this system even after annealing at 800°C. Figure 3 shows the XRD spectra of Cu (50 nm)/Ta/TaN/Ta/SiO₂/Si system, before and after annealing. In contrast to the previous case, the as-deposited sample exhibits Cu(111), TaN(111), and Ta(110) peaks. The intensity of Cu(111) peak also increased with increasing annealing temperature, and a TaN(200) peak became visible after annealing at 700°C. It is also noticed that the TaN(111) peak gradually shifted to the right and the Ta(110) peak gradually shifted to the left after annealing at 400 and 500°C. The Ta(110)

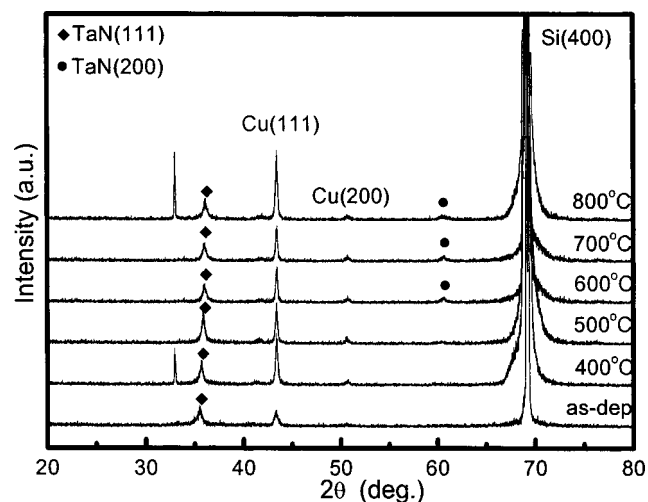


Figure 2. X-ray diffraction spectra of Cu (50 nm)/Ta/TaN/SiO₂/Si structure, as deposited and after annealing at various temperatures.

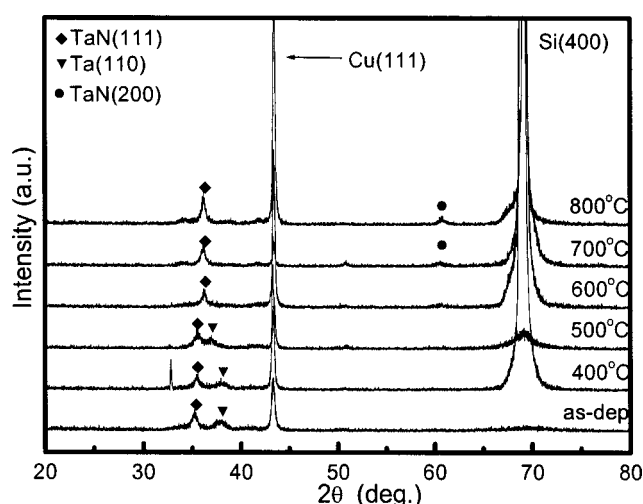


Figure 3. X-ray diffraction spectra of Cu (50 nm)/Ta/TaN/Ta/SiO₂/Si structure, as deposited and after annealing at various temperatures.

peak disappeared after annealing at 600°C or higher temperatures. The shift of TaN(111) and Ta(110) peaks might be attributed to the mixing of Ta/TaN/Ta layers, which results in the change of lattice parameters for TaN and Ta. No new phase is detected after annealing at 800°C. The characteristic XRD peaks of Cu (200 nm)/Ta/TaN/Ta/SiO₂/Si and Cu (200 nm)/Ta/TaN/Ta/SiO₂/Si systems, before and after various temperature annealing, are very similar to their parallel samples with thin copper thickness (50 nm). The shift of the TaN(111) peak and disappearance of Ta(110) peak are also found in the Cu (200 nm)/Ta/TaN/Ta/SiO₂/Si system. XRD results also reveal that the Cu/Ta(with or without)/Ta/TaN/SiO₂/Si structures remains thermally stable. The reaction products in Cu-Si metallization systems,^{19,20} such as Cu₃Si and TaSi₂, were not found in the current systems.

In order to confirm that shift of TaN(111) and Ta(110) peaks is due to the mixing of the Ta/TaN/Ta layers, the compositional depth profiles were examined by using AES. Figure 4 shows the AES depth profiles of Cu (50 nm)/Ta/TaN/Ta/SiO₂/Si system as deposited, and after annealing at 700°C. It can be seen that for the as-deposited samples, the Ta concentration was higher near by the Cu and SiO₂ layers (Fig. 4a), which corresponds to the Cu/Ta/TaN/Ta/SiO₂/Si layer structure. However, in Fig. 4b, the Ta concentration was almost a constant over the depth, indicating that the Ta/TaN/Ta structure was substituted by a single layer with uniform concentration of Ta. The result reveals that the Ta/TaN/Ta layer will mix after annealing at 700°C, and also confirms the merging of TaN(111) and Ta(110) peaks observed in XRD spectra.

Figure 5 presents the SEM micrographs of samples with thin (50 nm) copper layers after annealing at 600°C. Agglomerated copper islands were observed on the surface of 600°C annealed Cu (50 nm)/Ta/TaN/Ta/SiO₂/Si structure (Fig. 5a). On the contrary, the surface of Cu (50 nm)/Ta/TaN/Ta/SiO₂/Si remained continuous after annealing at 600°C (Fig. 5b). However, the copper surface was covered with fine particles so that the copper grains were difficult to identify. The surface morphology of thick Cu system remains continuous upon annealing, either with or without the Ta interlayer (is shown in Fig. 6). From the XRD and SEM analyses, we realize that the Cu/Ta (with or without)/Ta/TaN/SiO₂/Si structures remained chemically stable upon annealing. The abrupt increase of sheet resistance in Cu (50 nm)/Ta/TaN/Ta/SiO₂/Si system after annealing at 600°C is mainly due to the agglomeration of copper film. Sheet resistance values of the other three systems stay about the same upon annealing because the copper films remain continuous. To understand why the interposed Ta layer may prevent the copper agglomeration, further characterizations are shown as follows.

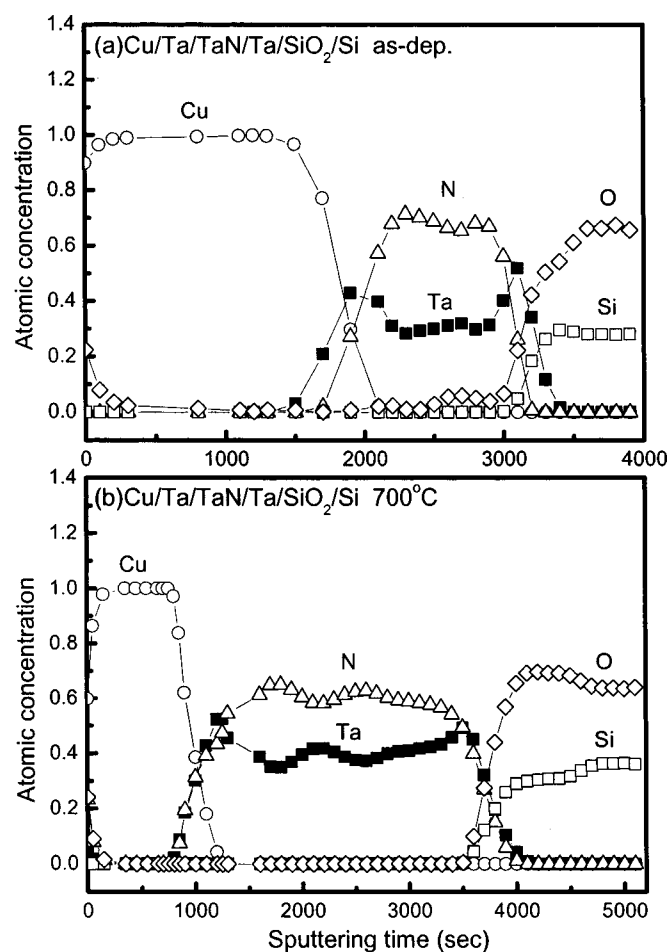


Figure 4. AES depth profiles of Cu (50 nm)/Ta/TaN/Ta/SiO₂/Si system (a) as deposited; (b) after annealing at 700°C.

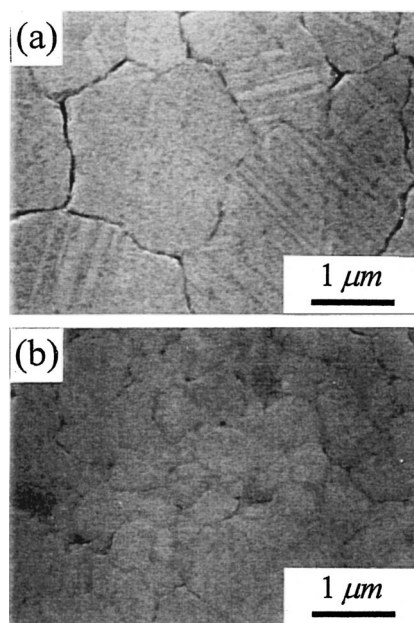


Figure 6. SEM micrographs of (a) Cu (200 nm)/Ta/TaN/Ta/SiO₂/Si, and (b) Cu (200 nm)/Ta/TaN/Ta/SiO₂/Si samples after annealing at 700°C.

Agglomeration of polycrystalline thin films were modeled into a three-step process:^{21,22} grain growth, formation of intergrain voids, and finally formation of agglomerated islands. Figure 7 shows the SEM micrographs of Cu (50 nm)/Ta/TaN/Ta/SiO₂/Si and Cu (50 nm)/Ta/TaN/Ta/SiO₂/Si systems after annealing at 800°C. Comparing with the micrograph of the 600°C annealed Cu (50 nm)/Ta/TaN/Ta/SiO₂/Si sample (Fig. 5a), it can be seen that the slightly connected islands in Fig. 5a became fully isolated islands upon annealing at 800°C (Fig. 7a). The surface of the Cu (50 nm)/Ta/TaN/Ta/SiO₂/Si system changed from a continuous layer after annealing at 600°C (Fig. 5b), to a surface with scattered voids after annealing at 800°C

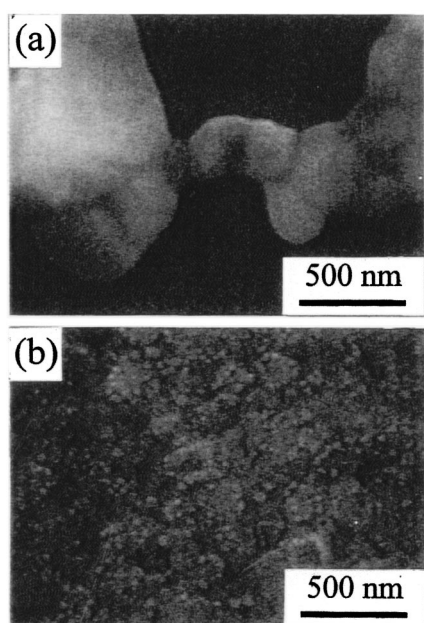


Figure 5. SEM micrographs of (a) Cu (50 nm)/Ta/TaN/Ta/SiO₂/Si, and (b) Cu (50 nm)/Ta/TaN/Ta/SiO₂/Si samples after annealing at 600°C.

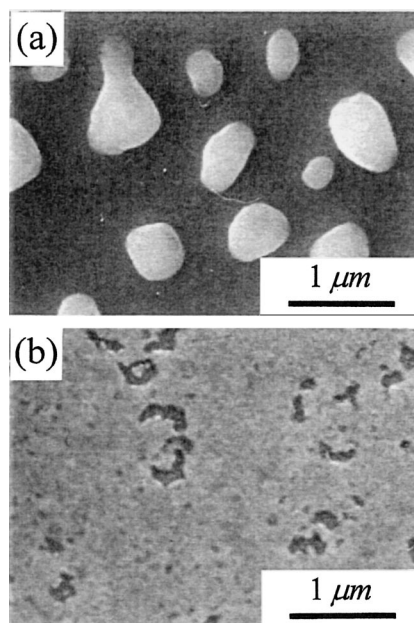


Figure 7. SEM micrographs of the (a) Cu (50 nm)/Ta/TaN/Ta/SiO₂/Si, and (b) Cu (50 nm)/Ta/TaN/Ta/SiO₂/Si samples after annealing at 800°C.

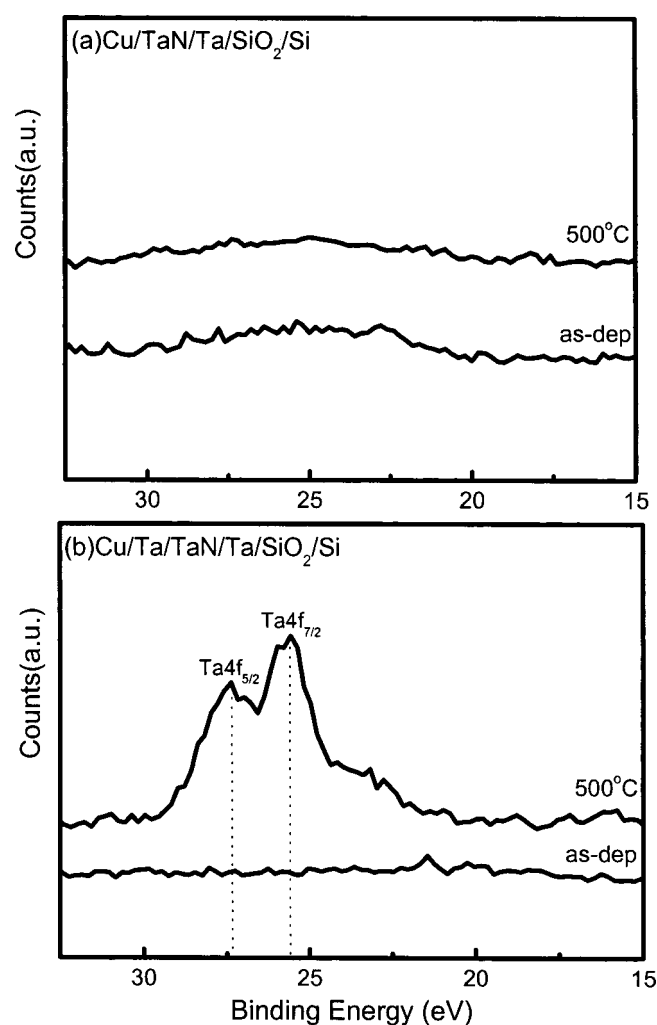


Figure 8. XPS spectra of Ta 4f core levels for the as-deposited and 500°C annealed samples of (a) Cu (50 nm)/TaN/Ta/SiO₂/Si, and (b) Cu (50 nm)/Ta/TaN/Ta/SiO₂/Si systems.

(Fig. 7b). The micrographs reveal that the agglomeration of copper thin film was delayed when a Ta interlayer is interposed between Cu and TaN.

Figure 6 shows the SEM micrographs of Cu (200 nm)/TaN/Ta/SiO₂/Si and Cu (200 nm)/Ta/TaN/Ta/SiO₂/Si systems after annealing at 700°C. The copper layer of both systems (with or without the Ta interlayer) remain nicely connected after annealing. The average grain size of copper in the 700°C annealed Cu (200 nm)/TaN/Ta/SiO₂/Si system was about 1.3 μm . However, the average grain size of copper in the 700°C annealed Cu (200 nm)/Ta/TaN/Ta/SiO₂/Si was 0.8 μm . It is obvious that grain growth of copper on a Ta layer between Cu and TaN system is retarded significantly. Consequently, the agglomeration of copper film becomes delayed, as shown in Fig. 7.

In addition to the delay of copper agglomeration, the surface of the 600°C annealed Cu (50 nm)/Ta/TaN/Ta/SiO₂/Si structure showed fine particles (Fig. 5b), which resembles reaction products. Figure 8 shows the XPS spectra of Ta 4f core levels for the Cu (50 nm)/TaN/Ta/SiO₂/Si and Cu (50 nm)/Ta/TaN/Ta/SiO₂/Si systems, as deposited and after annealing at 500°C. No Ta signal was detected on the surfaces of as-deposited and 500°C annealed Cu (50 nm)/TaN/Ta/SiO₂/Si (Fig. 8a). For the Cu (50 nm)/Ta/TaN/Ta/SiO₂/Si system, there was also no Ta signal detected on the as-deposited sample. However, after annealing at 500°C, two peaks were detected

in the XPS spectrum (Fig. 8b). The peaks are at the position of 27.4 and 25.5 eV, which close to the binding energies of 4f_{5/2} and 4f_{7/2} levels of Ta in Ta₂O₅.²³

Therefore, in a system with a Ta layer interposed between Cu and TaN, Ta will diffuse to the copper surface to form a tantalum-oxide (TaO_x) layer after annealing. However, no outdiffusion of Ta was observed for the system without a Ta interlayer. The outdiffusion of Ta can be attributed to the high affinity of Ta to oxygen; therefore, atoms in the Ta layer will outdiffuse to react with the residual oxygen in the vacuum furnace during high temperature annealing. On the other hand, because TaN is a thermally stable compound, no outdiffusion of Ta atoms was observed when copper was deposited on TaN.

From the experimental results shown above, it is observed that copper agglomeration will be retarded significantly while a Ta interlayer is interposed between Cu and TaN. The effect of adding a Ta interlayer on preventing copper agglomeration can be attributed to two factors. First, from XPS analysis, it was found that after high temperature annealing, Ta will outdiffuse to the copper surface to form a TaO_x layer. The TaO_x may serve as a cap layer and restrict both the mass transportation in copper surface and the movement of copper grain boundaries.²⁴ Therefore, grain growth of copper will be delayed by the formation of the TaO_x cap layer. Second, on the way of diffusing to the copper surface, Ta atoms will move along the copper grain boundaries and they will become the impurities stuffing along the grain boundaries. As a result, the movement of copper grain boundaries will be restricted and the grain growth rate of copper is reduced. Due to the reduction of grain growth, copper agglomeration will be prevented with a Ta interlayer.

An additional factor for preventing copper agglomeration via the interposed Ta layer may be due to different interactions between Cu-Ta and Cu-nitride. Ekstrom *et al.*²⁵ had reported that the growth of Cu on clean W surface followed the layer-by-layer model, but island growth was observed for Cu on a nitrided W surface. The authors concluded that Cu-W interaction is thermodynamically more favorable than Cu-nitride interaction. Analogously, in our experiment, the interposed Ta layer may promote a strong Cu-Ta interaction, while the Cu-TaN interaction may be rather weak. Consequently, the Ta interlayer can prevent the agglomeration of copper. However, it had been reported that using copper alloy²⁶ and choosing different barrier materials (for example, TaSiN^{11,17}) also have the similar consequence in suppressing copper agglomeration. Therefore, interposing a Ta interlayer may not be the only way to improve the copper morphology.

Furthermore, no agglomeration was observed for thick (200 nm) copper films, either on TaN or on Ta, after annealing up to 700°C (Fig. 6) and 800°C (SEM not shown). Comparison of agglomeration behavior for thin-and-thick films has also been reported for Cu (15 and 30 nm) on SiO₂,¹⁸ and Pd (5 and 50 nm) on SiO₂.²⁷ Both studies agree that thick films are less easy to agglomerate than thin films after the same heat-treatment. The connection between film thickness and agglomeration is often related to the model proposed by Miller *et al.*²¹ and Rha *et al.*²² Based on the minimization of overall surface, interface and grain boundary energies, this model predicts that a polycrystalline film will break up into islands when the D/t (D : grain size; t : film thickness) ratio exceeds a critical value. However, in practice, agglomeration always starts with the formation of voids at some local sites (grain boundary vertices, where three grains meet), but is not a global process for all grains.

Figure 9 shows the SEM micrograph of the 500°C annealed Cu (50 nm)/TaN/Ta/SiO₂/Si sample. The Cu film stayed mostly continuous but with voids scattered on the surface. The average Cu grain size was about 0.2 μm , resulting a D/t ratio of 4. The Cu film became agglomerated in the next heating stage (600°C, see Fig. 5a) but the Cu islands were still connected. One needs to anneal the sample at higher temperature to obtain the fully isolated islands (800°C, see Fig. 7a). On the other hand, the 700°C annealed Cu (200 nm)/TaN sample showed a continuous surface with no void, and the average Cu grain size was about 1.3 μm (see Fig. 6a), which

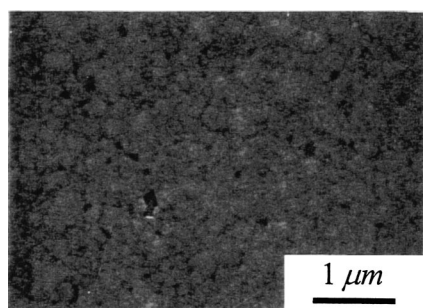


Figure 9. SEM micrograph of Cu (50 nm)/Ta/Ta/SiO₂/Si sample after annealing at 500°C.

corresponds to a D/t ratio of 6.7. Therefore, being deposited on identical substrates, the thick Cu films exhibited a greater D/t ratio than the thin Cu films before significant agglomeration occurs. The Miller/Rha model thus may be too simplified for practical situations.

Following our observation, we believe that agglomeration should be analogized to “phase transformation.” It starts with the nucleation of voids at some grain boundary vertices and followed by growth of voids, which gradually leads to the agglomerated islands. Based on the classic phase transformation theory, the nucleation rate is determined by the concentration of nuclei of the critical size and the collision frequency of atoms (or molecules) with nuclei.^{28,29} This can be expressed as

$$\dot{N} = \left[n_0 \exp\left(-\frac{\Delta G^*}{kT}\right) \right] \left[\omega_0 \exp\left(-\frac{\Delta G_M}{kT}\right) \right]$$

where n_0 =number of probable sites for nucleation, ΔG^* =critical Gibbs free energy for formation of a stable nucleus, ω_0 =a factor including vibration frequency of atoms and the area of the nucleus, and ΔG_M =the activation energy for the movement of atoms to the nucleus.

Here the “nuclei” may represent the voids for initiation of agglomeration. Grain size of thin film is normally smaller than that of thick films. Therefore, in thinner films, there are more grain boundary vertices (per unit area) to serve as the potential sites for nucleation of voids (*i.e.*, large n_0). In addition, ΔG^* is proportional to the volume of the critical nucleus^{28,29} and the ΔG^* value should be smaller for thin films because the critical void radius is in proportion to the film thickness.^{30,31} On the contrary, ω_0 may be larger for thick films (because of larger void area) and ΔG_M should be independent of the film thickness.

If the n_0 and ΔG^* values dominate the function, the nucleation rate of voids will be higher for thin film than for thick films, at the same temperature. That explains the difficulty of agglomeration for thick films, in addition to the “critical D/t ” requirement. From the previous study,¹⁷ it was observed that copper with a thickness of 10 nm and deposited on Ta barrier would agglomerate after annealing at 400°C. The result is in accordance with the mechanism that we have mentioned. That is, with the decrease of copper thickness, copper may agglomerate on Ta/TaN although no agglomeration was seen for 50 nm thick Cu on Ta/TaN. Nevertheless, the detailed mechanism for nucleation and grain growth of voids in copper films is yet to be explored.

Conclusion

The experiment demonstrates that copper agglomeration occurs only when the copper film is 50 nm in thickness and deposited

directly on TaN. Once a thin Ta layer is interposed between Cu and TaN, Ta atoms outdiffuse to the Cu surface and form a TaO_x cap layer. The TaO_x cap layer and Ta atoms diffusing along the Cu grain boundaries will retard the grain growth of copper. Consequently, the agglomeration of copper is prevented. With a thick (200 nm) Cu film, agglomeration is not observed in either Cu/TaN or Cu/Ta/TaN system even if annealed at 800°C. The absence of agglomeration for thick Cu films may be attributed to the lower nucleation rate of voids, as compared to the thinner Cu films.

Acknowledgments

The authors gratefully acknowledge the financial support from the National Science Council of Taiwan, R.O.C. (contract no. NSC-89-2216-E-006-037).

National Cheng Kung University assisted in meeting the publication costs of this article.

References

1. J. Tao, N. W. Cheung, and C. M. Hu, *IEEE Electron Device Lett.*, **14**, 554 (1993).
2. T. Nitta, T. Ohmi, T. Hoshi, S. Sakai, K. Sakaibara, S. Imai, and T. Shibata, *J. Electrochem. Soc.*, **140**, 1131 (1993).
3. E. R. Webber, *Appl. Phys. A: Solids Surf.*, **30**, 1 (1983).
4. J. D. McBrayer, R. M. Swanson, and T. W. Sigmon, *J. Electrochem. Soc.*, **133**, 1242 (1986).
5. S. W. Russell, S. A. Rafalski, R. L. Spreitzer, J. Li, M. Moinpour, F. Moghadam, and T. L. Alford, *Thin Solid Films*, **262**, 154 (1995).
6. H. Ono, T. Nakano, and T. Ohta, *Appl. Phys. Lett.*, **64**, 1511 (1994).
7. K. Holloway, P. M. Fryer, C. Cabral, Jr., J. M. E. Harper, P. J. Bailey, and K. H. Kelleher, *J. Appl. Phys.*, **71**, 5433 (1992).
8. F. Brand, J. Torres, J. Palleau, J. L. Mermet, and M. J. Mouche, *Appl. Surf. Sci.*, **91**, 251 (1995).
9. R. Kröger, M. Eizenberg, E. Rabkin, D. Cong, and L. Chen, *J. Appl. Phys.*, **88**, 1867 (2000).
10. J. Y. Lee, S. R. Jeon, and J. W. Park, *J. Mater. Sci. Lett.*, **15**, 1495 (1996).
11. T. Hara, K. Sakata, and Y. Yoshida, *Electrochem. Solid-State Lett.*, **5**, C41 (2002).
12. J. Li, J. W. Strane, S. W. Russell, S. Q. Hong, J. W. Mayer, T. K. Marais, C. C. Theron, and R. Pretorius, *J. Appl. Phys.*, **72**, 2810 (1992).
13. M. T. Wang, Y. C. Lin, and M. C. Chen, *J. Electrochem. Soc.*, **145**, 2538 (1998).
14. J. T. No, J. H. O, and C. Lee, *Mater. Chem. Phys.*, **63**, 44 (2000).
15. J. S. Chen and J. L. Wang, *J. Electrochem. Soc.*, **147**, 1940 (2000).
16. S. J. Wang, H. Y. Tsai, S. C. Sun, and M. H. Shiao, *J. Electrochem. Soc.*, **148**, G500 (2001).
17. T. Hara, K. Sakata, A. Kawaguchi, and S. Kamijima, *Electrochem. Solid-State Lett.*, **4**, C81 (2001).
18. J. W. Hartman, H. Yeh, H. A. Atwater, and I. Hashim, *Mater. Res. Soc. Symp. Proc.*, **564**, 257 (1999).
19. G. S. Chen and S. C. Huang, *J. Electrochem. Soc.*, **148**, G424 (2001).
20. M. H. Tsai, S. C. Sun, C. E. Tsai, S. H. Chuang, and H. T. Chiu, *J. Appl. Phys.*, **79**, 6932 (1996).
21. K. T. Miller, F. F. Lange, and D. B. Marshall, *J. Mater. Res.*, **5**, 151 (1990).
22. J. J. Rha and J. K. Park, *J. Appl. Phys.*, **82**, 1608 (1997).
23. C. D. Wagner, W. M. Riggs, L. E. Davis, J. F. Moulder, and G. E. Muilenberg, *Handbook of X-Ray Photoelectron Spectroscopy*, Perkin-Elmer Corporation (1979).
24. S. Y. Lee, R. E. Hummel, and R. T. DeHoff, *Thin Solid Films*, **149**, 29 (1987).
25. B. M. Ekstrom, S. Lee, N. Magtoto, and J. A. Kelber, *Appl. Surf. Sci.*, **171**, 275 (2001).
26. C. P. Wang, S. Lopatin, A. Marathe, M. Buynoski, R. Huang, and D. Erb, in *Proceedings of the IEEE International Interconnect Technology Conference 2001*, p. 86 (2001).
27. M. Eriksson, L. Olsson, U. Helmersson, R. Erlandsson, and L.-G. Ekedahl, *Thin Solid Films*, **342**, 297 (1999).
28. D. V. Ragone, *Thermodynamics of Materials*, Vol. II, Chap. 6, John Wiley & Sons, New York (1995).
29. D. A. Porter and K. E. Eastering, *Phase Transformation in Metals and Alloys*, Chap. 4 and 5, Chapman and Hall, London (1981).
30. D. J. Srolovitz and S. A. Safran, *J. Appl. Phys.*, **60**, 247 (1986).
31. D. J. Srolovitz and S. A. Safran, *J. Appl. Phys.*, **60**, 255 (1986).